Available online at www.sciencedirect.com

jmr&t Journal of Materials Research and Technology

journal homepage: www.elsevier.com/locate/jmrt

Original Article

# Mechanical and wear behaviors of 316L stainless steel after ball burnishing treatment

Selma Attabi [a,*], Abdelaziz Himour [a,**], Lakhdar Laouar [b], Amir Motallebzadeh [c]

[a] Metallurgy and Materials Engineering Laboratory (LMGM), University Badji Mokhtar of Annaba, BP 12, 23000 Annaba, Algeria

[b] Laboratory of Industrial Mechanics (LMI), Badji Mokhtar – University of Annaba, PO Box 12, 23000 Annaba, Algeria

[c] Koç University Surface Science and Technology Center (KUYTAM), Rumelifeneri Yolu, 34450 Sariyer, Istanbul, Turkey

ARTICLE INFO

*Article history:*
Received 3 July 2021
Accepted 20 September 2021
Available online 30 September 2021

*Keywords:*
Ball burnishing
Microhardness
Wear
Friction
316L SS

ABSTRACT

The performance and durability of orthopedic implants are mainly determined by their surface integrity. Ball burnishing (BB) is a kind of finishing treatment which improves the surface dependant mechanical properties of metallic biomaterials. In this work, this process was applied on the flat surface of 316L stainless steel to enhance its microhardness and wear resistance. The mathematical modeling of microhardness Vickers was performed by the response surface method (RSM) based on Box–Behnken plans, and the optimum regime was applied under several passes to investigate the effect of number of passes (*i*) on the surface properties. The evolution of microhardness, nano-hardness and elastic modulus was then examined. Wear resistance, in terms of variation of Coefficient of friction and wear loss, was also investigated. Finally, XRD analysis was performed to evaluate any change in structure produced by BB. The results show that burnishing treatment permits to raise the microhardness by up to 38.3% and to reduce the wear loss by up to 65.2%. Nano-hardness and elastic modulus were also increased after application of the process. XRD patterns indicate that grain refinement was induced with no change in phases composition. The number of passes is proved effective in increasing the depth of the hardened layer, which influences subsequently on the frictional behavior of 316L stainless steel.

© 2021 The Author(s). Published by Elsevier B.V. This is an open access article under the CC BY-NC-ND license (http://creativecommons.org/licenses/by-nc-nd/4.0/).

## 1. Introduction

In orthopedic applications, a great interest is directed to the control of surface properties of mechanical parts. Joints of total hip replacements are widely made of 316L austenitic stainless steel (SS) [1] and are permanently subjected to friction movements [2]. However, this stainless steel exhibits a poor wear resistance which limits its applications in this field [3]. Mechanical surface treatments like shot peening and burnishing are increasingly applied on biomedical parts to achieve the high requirements of surface finishing, surface hardness, wear

* Corresponding author.
** Corresponding author.
E-mail addresses: attabi.selma@gmail.com (S. Attabi), ahimour@yahoo.fr (A. Himour).

https://doi.org/10.1016/j.jmrt.2021.09.081

2238-7854/© 2021 The Author(s). Published by Elsevier B.V. This is an open access article under the CC BY-NC-ND license (http://creativecommons.org/licenses/by-nc-nd/4.0/).

resistance, and fatigue durability [4]. Ball burnishing (BB) has been widely tested to improve the wear resistance of materials by reducing their surface roughness and raising their microhardness [2,4–6]. This cold finishing treatment is based on the plastic deformation of surface asperities by pressing a hard ball along the workpiece surface [7,8]. Compressive stresses are thus induced in the deformed layer accompanied with strain hardening, which produces a harder surface [9]. This easy-fast process enhances accordingly wear resistance of rubbing surfaces and expands their long-term properties.

Ball burnishing have approved its efficiency on several types of materials when appropriate parameters are used. Revankar et al. [10] optimized the ball burnishing process applied on Ti–6Al–4V titanium alloy using Taguchi method. They have stated that a combination of medium burnishing speed, low feed, low burnishing force with three passes is helpful for reduced surface roughness (77%), whereas burnishing with medium speed and feed, higher force and more number of tool passes could improve the surface hardness (17%). In later study [6], the same researchers evaluated the wear resistance of Ti–6Al–4V after ball burnishing. Experiments carried out with medium burnishing speed, low feed, high burnishing force and three passes permitted to minimize the specific wear rate (52% decrease), whereas the use of medium speed, low feed, medium force and two numbers of passes could minimize the coefficient of friction (64% decrease). Dimitrov et al. [11] conducted ball burnishing under a new kinematic scheme to evaluate its effect on hardness and phase composition of surface layer of AISI 304L stainless steel. The results have indicated that the surface hardness was increased with about 50% and the depth of the hardened layer could attain 500 μm. However, it was recommended to use a low force combined with high number of passes to prevent the formation of strain induced martensite. Teimouri et al. [12] have evaluated the surface properties of 6061-T6 aluminum alloy subjected to ultrasonic assisted ball burnishing. Results have showed that simultaneous minimization of surface roughness and maximization of hardness could be attained when ultrasonic vibration amplitude of 8 μm, feed rate of 1000 mm/min and static force of 38 N, were selected. Jerez-Mesa et al. [13] analyzed the surface integrity of ball-end milled Ti–6Al–4V surfaces through vibration-assisted ball burnishing. The experiments have indicated that the combination of 350 N, 5 passes and 900 mm/min has lead to the best enhancement of surface topology, hardness and residual stresses. It was also observed that applying five passes along the same direction during BB process allows to achieve a residual hardening from around 100 to 500 μm deep layers. Świrad et al. [14] investigated the influence of hydrostatic burnishing strategies (raster and spiral techniques) and burnishing parameters on the roughness of X38CrMoV5-1 steel. They have reported that the raster strategy in the burnishing of curved shapes surfaces is recommended due to the obtained stability of process. Silva-Álvarez et al. [15] proposed to use the ball burnishing process on the CoCrMo alloy to improve its surface properties. Factorial design of experiments (DoE) have showed that force is the most significant factor that influences on the surface quality. It was also reported that the appropriate combination of process parameters allowed to raise the hardness by 41.4%, reduce the roughness by 72.7% and minimize the corrosion rate by 92.4%. Nguyen et al. [16] applied the burnishing process on H13 steel to decrease the mean roughness and raise the Brinell hardness. According to the machining parameter-based optimization followed, the use of 719 Rpm burnishing speed, 431 mm/min burnishing feed, 0.12 mm depth of penetration, and 3 numbers of rollers could decrease the mean roughness depth by 7.83% and increase the Brinell hardness by 29.61%. The optimum results showed that the energy consumption could be also decreased by 39.50%. Basak et al. [17] studied the effect of ball burnishing on the surface roughness, microhardness, and the strength of 5083 Al–Mg material. They have revealed that the burnishing force and feed rate are the most significant parameters for reducing the surface roughness and increasing the surface hardness. Kalisz et al. [18] examined the surface integrity and tribological characteristics of $AlCu_4$-MgSi aluminum alloy after sequential ball end milling-burnishing process of curvilinear surfaces. The results have showed that burnishing process have produced super finished surfaces with almost two-fold reduction of volumetric wear rate. Cagan et al. [19] investigated the effect of burnishing environments on surface quality of AZ91D magnesium alloy. They revealed that the better surface roughness values were generated by using boron oil as environment. Higher force (400 N), low feed rate (0.05 mm/min) and 3 number of passes were selected as the optimum factors for decreasing the surface roughness. Charfeddine et al. [20] studied the application of grinding and ball-burnishing simultaneously on AISI 4140. Their results have shown that combined grinding/ball-burnishing affects a more important workpiece depth (2.7 mm) exceeding the depth obtained by thermochemical surface treatments. Jerez-Mesa et al. [21] compared between the effects of vibration-assisted ball burnishing process and its non-vibration assisted version on the surface properties of AISI 301LN alloy. The results have mentioned that the application of ball burnishing produces the higher effect on annealed AISI 301LN (containing an original contents of 3% of martensite) by achieving a residual hardening to 250 μm down and an increased hardness of the immediate surface in almost 65%. The study revealed that no conspicuous effect of the application of vibration assistance was observed.

Some researchers have investigated the effect of ball burnishing on surface properties of 316L SS. Lee et al. [22] used Taguchi method to optimize the ball burnishing process and they have reported that surface roughness of 316L can be reduced from 2 μm to 0.6 μm when the following parameters are fixed: ball material $ZrO_2$ or SiC; depth of penetration 16–20 μm; feed 95–125 μm, burnishing speed 300–320 mm/min with either kerosene, machine oil or engine oil used as the lubricant. Yilmaz and Sadeler [23] also explored the influence of BB on the surface integrity of 316L. They revealed that the process can reduce the surface roughness of the stainless steel by 50% and raise its hardness by 36% to a depth of 180 μm. In Gulhane et al.'s study [24], the full factorial design (DOE) was used to evaluate the influence of BB parameters on surface roughness of 316L SS, and it was stated that higher number of passes is required at higher pressure in order to achieve an improvement of 85% in surface roughness. Tanaka et al. [25] have recorded that high compressive residual stresses of 700 MPa were generated in the burnished layer of

316L SS, and an amelioration of hardness by 100 Hv was detected. Salmi et al. [26] applied ultrasonic burnishing on Co–Cr and 316L SS samples made by additive manufacturing. They performed an analysis of variance (ANOVA) to study the effect and interactions of process parameter on the final surface quality. The experiments showed that ultrasonic burnishing of 316L requires 1000 mm/min for the feed speed, 0.025 mm for the side shift and 1 mm for spring compression to reduce the surface roughness by approximately 13 times and increase the microhardness by 70.7%. It is worth mentioning that the aforementioned works are in fact restricted to the evaluation of BB on the outcome of surface integrity parameters, particularly surface roughness and hardness. However, relating these parameters with the improvement of the functional responses of the workpiece, such as its wear behavior, is often overlooked. It is hence necessary to evaluate whether ball burnishing shows good effects when applied on 316L SS in terms of mechanical properties and wear resistance such that the process can be applied to ameliorate the durability of orthopedic parts.

The aim of this work is to investigate the impact of ball burnishing on surface quality and wear resistance of 316L SS used for joint prosthesis manufacturing. Response surface method (RSM) based on Box–Behnken design [27] is used to optimize the microhardness of studied alloy. Under the optimum regime fixed, series of BB were conducted with varying the number of passes (i) to establish its effect on the tribological behavior of 316L SS.

## 2. Materials and technical methods

### 2.1. Material

Austenitic stainless steel 316L SS manufactured by Roldan S.A (Spain) was employed for the experiments. Its chemical composition determined by atomic adsorption revealed: the wt-% is 0.02% C, the wt-% is 16.64% Cr, the wt-% is 10.35% Ni, the wt-% is 2.03% Mo and the rest is Fe. Mechanical properties of a cylindrical bar are: Re: 575 MPa, Rm: 707 MPa, A: 35% and 235 Hv.

### 2.2. Sample preparation and ball burnishing

The workpiece was cut from the raw material as 30 mm in diameter and 400 mm in length. Its flat surface was pre-machined on TOS TRENSIN, model SN40 lathe with 6.6 kW power on the spindle using a P10 carbide cutting tool. A feed rate "$f_t$" of 0.037 mm/min, depth of pass "p" of 1 mm, and rotational frequency of piece "N" of 560 rev/min, were fixed as the parameters of pre-machining for all specimens. After turning, ball burnishing was accomplished on the same lathe by means of specific device. This last is designed such as a 100C6 hard ball, to which an adjustable transversal charge ($P_x$) is transferred, rotates in all directions and impacts continuously the flat surface of workpiece. The operation was conducted with rotation frequency of 560 rev/min, one pass and under lubrication. The plastic deformation of the surface result from the combination of the applied charge on the ball and the feed rate.

### 2.3. Methodology and experimentation

Because hardness is a relevant factor that controls the wear resistance of mechanical parts [16,17], surface microhardness of 316L SS was firstly optimized using response surface method (RSM). Box–Behnken design was hence employed to optimize the burnishing parameters with minimizing the number of experiments and assuring the prediction accuracy. The applied approach based on Box–Behnken plan represents the possibility of studying a lot of factors at three levels for each factor, with the minimum of experiments number. It allows to use a mathematical model of second degree, which makes it possible to analyze the effect of each factor as well as the effect of the interaction between the factors on the response. This plan helps also in the organization and processing of tests with respecting certain real conditions of the experiments. However, the fixed approach requires a limited number of experiments because of several reasons. The tests must be adapted to the kinematic chain of the machine which does not permit a continuous presentation of inputs (such as feed and speeds), and therefore the plan that had to be retained should not contain a large number of levels. The tests are also adapted to some experimental restrictions such as material limitation which demand that certain tests cannot be carried out because certain levels cannot be reached. The design of experiments based on BOX BEHNKEN method, used in this study, is flexible enough to comply with all these restrictions [27].

Three process inputs (charge "$P_x$", feed rate "$f$" and ball diameter "D") were selected with three levels (−1, 0, +1). The range of variation of each parameter was determined based on previous references [28], preliminary experiments and workpiece properties (elongation %, hardness, dimensions). The fixed levels and their associated values are listed in Table 1. After designing the experiments in respect to the experimental matrix, the experiment process was conducted on the outcome of microhardness Vickers "Hv". The predictive model expressing the relation between the microhardness Vickers "Hv" and the process parameters ($P_x$, $f$, D) was then obtained. Subsequently, the optimum parameters that produce the optimum microhardness were used to conduct a second series of experiments where the number of passes "i" was varied by up to $i = 5$.

### 2.4. Characterization

The surface microhardness of pre-machined and burnished samples was measured by means of Innovatest microdurometer. All tests were carried out using a load of 100 Kgf applied during 10 s. The average diameters of five indentations were calculated to get a reliable data. Nano-mechanical

**Table 1 – Ball burnishing input parameters and their associated values.**

| Input parameter | Levels | | |
|---|---|---|---|
| | −1 | 0 | +1 |
| X1: Charge $P_x$ (N) | 80 | 160 | 240 |
| X2: Feed rate $f$ (mm/rev) | 0.065 | 0.124 | 0.18 |
| X3: Ball diameter $D$ (mm) | 7 | 10 | 13 |

**Table 2 – Microhardness values of burnished surfaces.**

| Experience | $P_x$ (N) | $f$ (mm/tr) | $D$ (mm) | Microhardness (Hv) |
|---|---|---|---|---|
| 01 | 80 | 0.065 | 10 | 455.2 |
| 02 | 240 | 0.065 | 10 | 350.6 |
| 03 | 80 | 0.18 | 10 | 542.2 |
| 04 | 240 | 0.18 | 10 | 368.1 |
| 05 | 80 | 0.124 | 7 | 398.8 |
| 06 | 80 | 0.124 | 13 | 432.2 |
| 07 | 240 | 0.124 | 7 | 442.2 |
| 08 | 240 | 0.124 | 13 | 528.2 |
| 09 | 160 | 0.065 | 13 | 468.7 |
| 10 | 160 | 0.18 | 7 | 451.1 |
| 11 | 160 | 0.065 | 7 | 462.3 |
| 12 | 160 | 0.18 | 13 | 449.3 |
| 13 | 160 | 0.124 | 10 | 409.5 |
| 14 | 160 | 0.124 | 10 | 483.0 |
| 15 | 160 | 0.124 | 10 | 445.5 |

properties including nanohardness and elastic modulus were determined using Instrumented nano-indentation (Agilent G200, USA) test with a trigonal Berkovich indenter. Measurements were carried out under the continuous stiffness measurement (CSM) option with applying a maximum load of 450 mN, a maximum depth of penetration of 500 μm, and a holding time of 5 s. Because the nanoindentation test is extremely sensitive to the impurities present in the material as well as to the roughness, around thirty indentations at different regions on the surface of each sample were carried out, and the average of their values was retained.

Wear tests carried out on a pin-on-disk tribometer (TRC, module 4.5 Q), were proceeded to investigate the wear performance of burnished surfaces. Dry sliding tests were assessed using alumina ball $Al_2O_3$ of 6 mm diameter fixed against the disk of 316L SS (ø15 × 8 mm thickness). A normal load of 10 N and a constant velocity of 5 cm/s were fixed along 1800 tours. Environmental temperature and humidity of all tests were maintained at 25 °C and 30%, respectively. After the test, both Zeiss Ultra Plus field emission scanning electron microscope and Altisurf500 profilometer were used to characterize the worn surfaces.

X-ray diffraction (XRD) measurements were performed on 316L SS surface before and after ball burnishing to evaluate any changes in structure. Bruker Advance D8 X-ray diffractometer with Cu-kα radiation (1.5418 Å) was used at a scan speed of 0.02°/s.

## 3. Results and discussion

### 3.1. Effect of BB on surface microhardness

Table 2 shows the microhardness values before and after the application of BB treatment. It can be noted that the microhardness of the burnished samples was in the range of 350.6–542.2 Hv as compared to the turned sample whom hardness was measured as 323.4 Hv. These results show that BB process has a positive impact on strain hardening of 316L which is identified by an improvement of surface microhardness ranging between 08.4 and 67.6%. The best hardening produced was obtained by the application of the minimum load (80 N), the maximum feed (0.18 mm/rev) and the medium ball (10 mm). If the same ball is used with increasing the load to its maximum or reducing the feed to its minimum, the microhardness Hv is reduced, as shown by comparison between experiments 03/04 and 01/03, respectively. Hence, it can be suggested that high feed rates and low charges are more favorable to get the best work hardening of 316L SS surface. Moreover, it can be noted that the effect of ball size is almost insignificant when low and medium charges are applied, which can be revealed from comparison between experiences 05/06; 09/11; 10/12. However, when high charge is applied, the biggest ball has provoked higher effect of work hardening as compared to the smallest ball (experiences 07/08).

In response surface methodology (RSM), the studied response Y is represented by a properly adjusted mathematical model. Nonlinear prediction models are actually required to find the best correlation between the mathematical models and experimental results [29]. In the present study, an algorithm developed by Laouar et al. [30] was used to carry out data treatment. Box–Behnken plan was followed to generate a nonlinear model of second degree (Eq. (1)) whom the interactions are of second order [29].

$$\widehat{Y} = a_0 + a_1.X_1 + a_2.X_2 + a_3.X_3 + a_{12}.X_1.X_2 + a_{13}.X_1.X_3 + a_{23}.X_2.X_3 + a_{11}.X_1^2 + a_{22}.X_2^2 + a_{33}.X_3^2 + e \quad (1)$$

with $\widehat{Y}$ is the theoretical developed response and $e$ is the error of the model.

The relationship between the microhardness and the different ball burnishing parameters (Eq. (2)) is established through the numerical resolution of Eq. (1):

$$\widehat{Hv} = 445.6667 + 17.4875.X_1 + 9.2375.X_2 + 15.575.X_3 - 17.375.X_1.X_2 + 13.X_1.X_3 + 2.05.X_2.X_3 + +11.9958.X_1^2 + 4.6458.X_2^2 + 16.8292.X_3^2 + e \quad (2)$$

where $\widehat{Hv}$ is the theoretical developed microhardness Vickers and e is the error of the model. Statistical evaluation of this model has resulted in: a coefficient of correlation $R^2 = 0.99$, and a coefficient of Fisher $F_{cal} = 6.4 < F_{theo} = 19.2$, which indicates that the model is well adjusted according to Spiegel [31].

### 3.2. Effect of burnishing process parameters

The effect of the different parameters and their interactions are represented in Fig. 1. The curves describe the variation of the response (Hv) as a function of $P_x$ and $f$ for the three balls used. It appears from the analysis of these curves that the microhardness Hv has the same evolution as a function of $P_x$ and $f$ for the three ball sizes. At small and medium ranges of force, the increase in feed rate leads to the increase of microhardness achieving almost 480 Hv for the ball with $D_b = 10$ mm and 490 Hv for both balls with $D_b = 7$ mm and $D_b = 13$ mm. However, at high loads, the increase in fee rate affects the microhardness where a decrease of Hv is observed for the three ball sizes. Consistently with analysis of Table 2, it can be suggested that, whatever the size of the ball, the

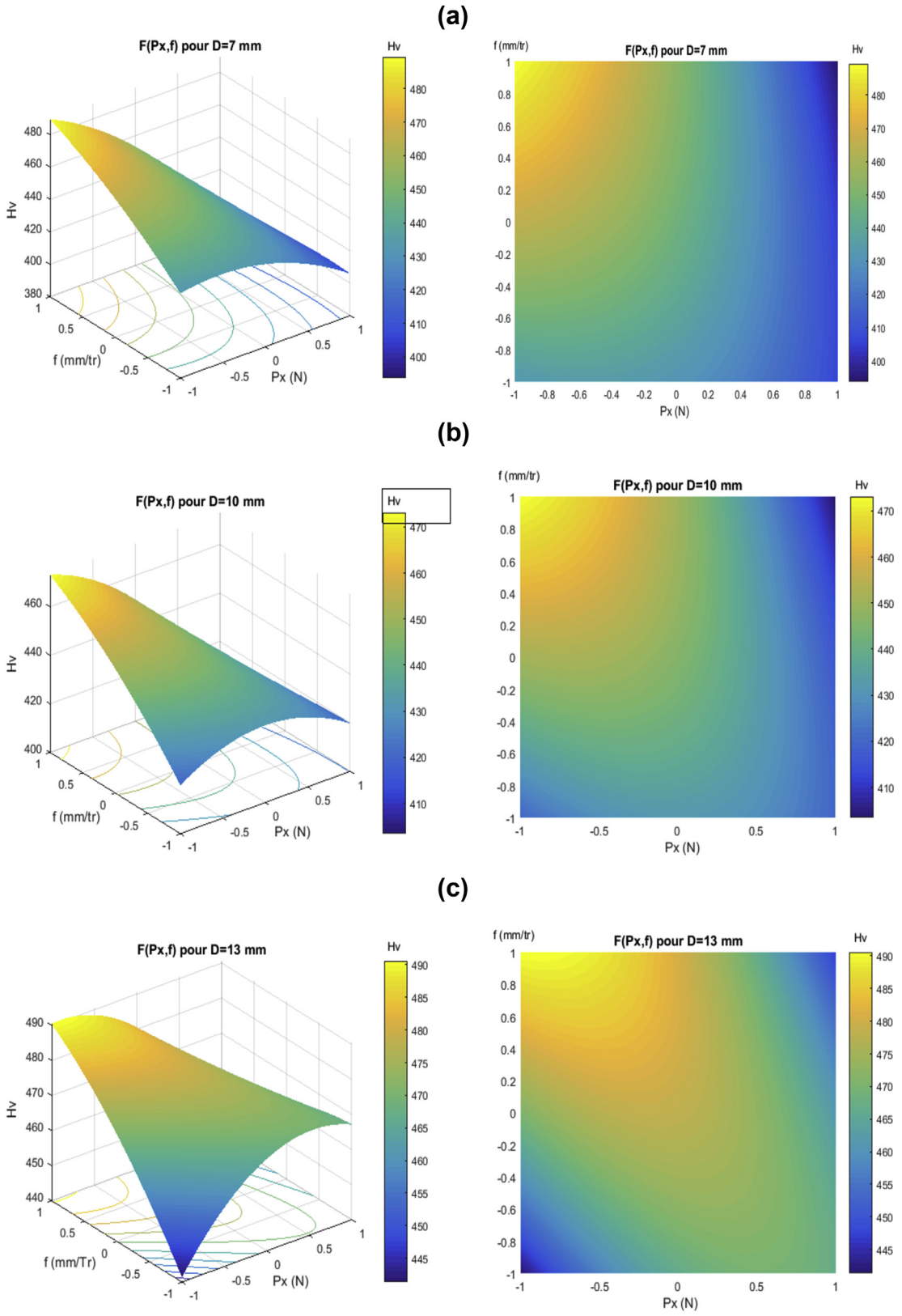



**Fig. 1 – Variation of microhardness Hv in respect to $P_x$ and $f$: (a) $D_b = 7$ mm; (b) $D_b = 10$ mm; (c) $D_b = 13$ mm.**

highest feed rate $f$ associated with the lowest load is always required to get greater work hardening of the surface, otherwise, a negative effect on surface hardness is produced. Nguyen and Le [32] have revealed the same observation and attribute it to the higher material plasticity and work hardening generated by the increment in process parameters.

According to Bourebia et al. [28], the axial force is more dominant in front of the radial component when low burnishing pressure is applied allowing better deformation of the surface. It also appears that the microhardness tends to decrease with the combination of low feed rate ($f$) with high load ($P_x$) more significantly for the 7 mm and 10 mm ball diameters (Fig. 1a and b) compared to the 13 mm ball diameter (Fig. 1c). This could be explained by the fact that the surface of contact of the ball with 13 mm of diameter is much higher as compared to the balls with 7 mm and 10 mm. Therefore, during BB process, the plastic deformation induced by the penetration of the greatest ball covers a large surface which results in more work hardening on the surface, and thus higher values of micro-hardness can be attained [2]. Basak et al. [17] have found that the maximum ball diameter is more favorable to obtain the best hardness but the ball size has a secondary influence in comparison to burnishing force and feed rate. According to our results, the same statement can be declared since the values of microhardness reached for the biggest ball vary in the interval of [440 Hv–490 Hv], while it ranges between [400 Hv–475 Hv] for the medium and the small ball.

According to the mathematical model, optimum microhardness was determined as $Hv_{opt} = 490.6 \pm 84.32$ *Hv* with an optimal regime: $P_{opt} = 87.1$ *N*, $f_{opt} = 0.18$ *mm/tr*, and $D_{opt} = 13$ *mm*. When the fixed parameters were applied during BB process, measurement of microhardness revealed a real value "$Hv_{real}$" which is 447.3 Hv. This value belongs to the interval predicted by the model. Therefore, our model is well adopted to the experiments. In comparison to the untreated surface (323.4 Hv), the microhardness was raised by more than 100 Hv which shows the beneficial effect of ball burnishing on the hardening of 316L SS.

### 3.3. *Effect of number of passes on surface characteristics*

Because number of passes "i" in another relevant parameter which influences the surface hardness and accordingly the wear resistance of treated surfaces [6], it was varied by up to $i = 5$ when the optimum regime was applied ($P_{opt}$, $f_{opt}$, and $D_{opt}$) to establish its impact on 316L SS surface properties.

#### 3.3.1. *Effect of number of passes on surface microhardness*

Fig. 2 represents the variation of microhardness as a function of number of passes "i". The effect of increasing the number of passes is manifested by a variation in the final microhardness value. If raising the number of passes to $i = 2$ did not really cause a remarkable change in the microhardness as compared to $i = 1$, the use of number of passes between $i = 3$ and $i = 5$ generates a very significant hardening expressed by a microhardness ranging from 516.8 Hv for $i = 3$ to 593.0 Hv for $i = 5$, as it is showed in Fig. 2a.

The increase in microhardness after burnishing is due to the movement of the deforming ball. Indeed, the application of the load during burnishing promotes the ball to penetrate the surface, which causes, in the first place, an elastic deformation of the irregularities. When the elastic limit of the latter is reached, their plastic deformation takes place. This leads to an increase in the internal residual compressive stresses, which in turn cause a considerable increase in the hardness of the surface [and immediate sub-surface of the material [10,33]]. The increase of microhardness as number of passes increase is obvious because each repeated pass on the same workpiece increases the level of plastic deformation which induce more residual stresses in the burnished layer. Hence, each pass improves the surface microhardness. According to Hassan [33], the increase in number of passes during burnishing produces a condensed grain structure and raises the structural homogeneity, which results in an increase in the rate of work hardening. Similar effect of number of passes was reported in the literature [34–37]. However, the aforementioned studies report that the increase in microhardness will level off at high number of passes due to excessive cold working which can lead to failure. In our study, no saturation effect was observed even when the number of passes is raised to $i = 5$. This could be explained by the use of high feed rate and low load. Thus, the repeating action of ball burnishing on the same surface will not affect the layers already deformed regarding that the ball is moderately loaded and passes quickly. It was reported in the research of Basak et al. [17] that as the feed rate decreases, the burnishing time on the surface increases. Consequently, if low feed rate is combined with several passes, an excess of deformation time can be achieved and an excessive work hardening can be provoked.

Fig. 2 regroups also all the resulted burnished surfaces hardness depending on the depth in the material. A similar hardened surface layer up to 15 μm was detected for the samples burnished with $i = 1$, $i = 2$, and $i = 3$, as it is shown in Fig. 2b–d. When four passes are applied (Fig. 2e), a slight increase in the depth of the hardened surface was noted reaching 25 μm, while BB with five passes produced a hard layer with a thickness up to 40 μm as shown in Fig. 2f. Consistently with the results of Kalisz et al. [18], the recorded values of thicknesses indicate that the strain hardening penetrates only to about 40 μm beneath the surface.

#### 3.3.2. *Effect of number of passes on nano-hardness and elastic modulus*

Fig. 3a shows representative load–displacement curves of the untreated sample and also the burnished ones. Values of nano-hardness and elastic modulus determined by the nano-indentation test are also regrouped in Fig. 3b.

As outlined by A.W. Warren et al. [38], transition of the load–displacement curves to larger indentation depths indicates the presence of tensile stresses while its movement to smaller indentation depths refers to compressive stresses. Clearly, the load–displacement curves of all burnished samples are shifted 'left' in comparison to unburnished sample, suggesting that more compressive residual stresses were generated by ball burnishing treatment. Lang al [39] have attributed the difference of nano-hardness generated to strain hardening, size effect, grain refinement, and induced residual compressive stresses. Wang et al. [40] have reported that the increase in surface hardness is due to work hardening, which was commonly attributed to the formation of a large number of dislocations and deformation twins after mechanical surface treatment. It also appears in Fig. 3a that the curves of burnished samples show higher slopes than the curve of the untreated sample, suggesting that their modulus of elasticity is greater. Among the five burnished surfaces,

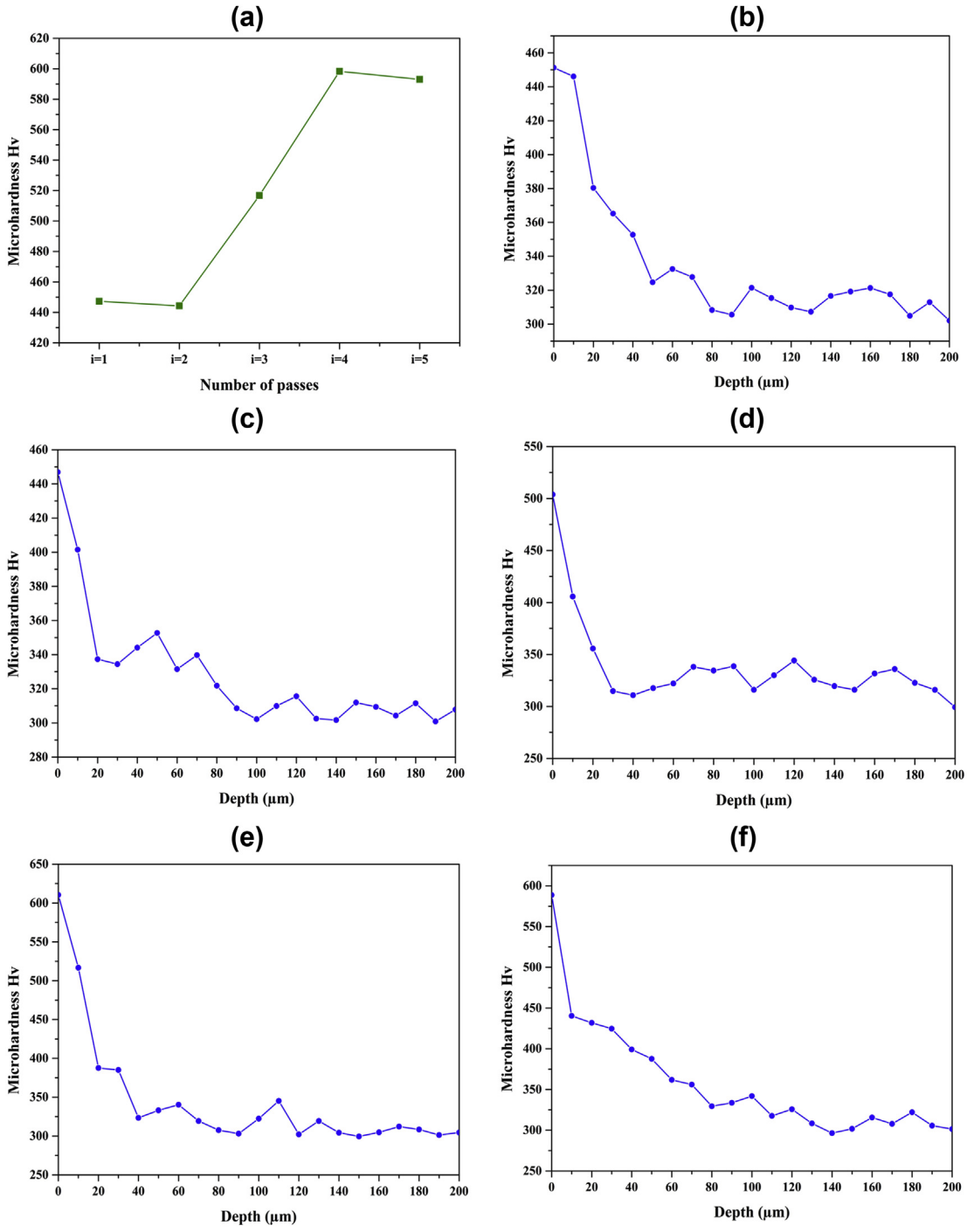



**Fig. 2 – Results of surface microhardness: (a) Microhardness Hv versus i; Variation of microhardness in depth for: (b) i = 1; (c) i = 2; (d) i = 3; (e) i = 4; (f) i = 5.**

the one treated with the optimal microhardness regime (i = 1) has the lowest Young's modulus (189.5 GPa), while the other surfaces have a similar Young's modulus ranging between [205.0–219.1 GPa] as shown in Fig. 3b. The same figure shows that the reference sample has the lowest elastic modulus which is found equal to 165.5 GPa. For nano-hardness, the curves in Fig. 3a indicate clearly that the treated surfaces are harder than the untreated one since their penetration depths are significantly lower. This is well consistent with Fig. 3b showing that the nano-hardness of the untreated sample is weaker as compared to the burnished ones, which is reasonably caused by the compressive residual stresses already discussed. Also, it should be noted that both nano-hardness and elastic modulus raise with the increasing of number of passes, which is due to the repetitive work hardening generated after each pass.

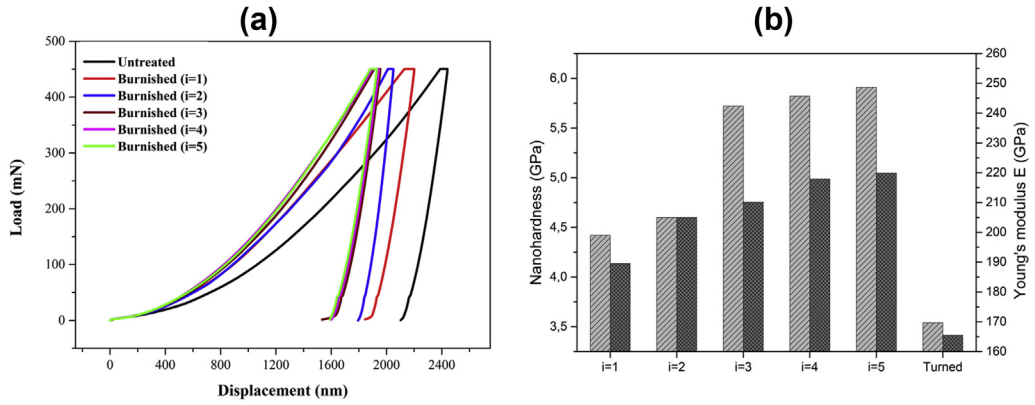



**Fig. 3 – Results of nano-indentation tests of all samples: (a) curves of load–displacement; (b) nano-hardness and elastic modulus values.**

3.3.3. *Effect of number of passes on wear resistance*

Representative plots of variation in the coefficient of friction (COF) in respect to the distance for all samples are shown in Fig. 4a. All the curves are characterized by successive three regions. In the first one, the COF increases immediately due to the plastic deformation of the surface asperities [41]. During the second step, a significant increase in the COF is detected then the steady-state is finally reached when the COF remains nearly constant. It appears from the curves that the second period of the curve corresponding to ($i = 1$) is longer compared to the other cases, indicating that the alumina ball had taken a longer time to deform the irregularities. This is ascribed by the high consolidation of the surface produced when the optimum regime is fixed during BB treatment. The variation of average COF and volumetric wear loss in respect to surface state are represented in Fig. 4b. Both COF and wear loss of the turned sample were the highest (0.584 and 3.48 $\times$ $10^{-4}$ $mm^3$/(N m)) in comparison to the burnished samples except the one burnished with ($i = 3$) which exhibited an increased COF (0.603) and almost unchanged wear rate (3.36 $\times$ $10^{-4}$ $mm^3$/(N m)). The sample burnished with one pass ($i = 1$) represented the best wear resistance characterized by an improved COF (0.501) and reduced wear rate (1.21 $\times$ $10^{-4}$ $mm^3$/(N m)). Hence, an improvement rate of wear rate reduction by up to 65.2% was registered. The enhancement in wear resistance is due to the increase in microhardness consistently with previously published works. Yasuhiro and Kei [42] have stated that the wear amount of beta-type titanium alloy is reduced when the microhardness is raised. AISI 316L has a poor tribological behavior because of its low hardness [43]. Thus, if the microhardness increases, wear resistance will accordingly increase. El-tayeb et al. [44] have reported that the wear resistance is dependent on the sub-surface properties of the material subjected to mechanical surface treatments like burnishing. The same statement was confirmed by Dzierwa et al. [5].

The effect of number of passes on the COF and the wear rate which could be established through the comparison between the results of burnished samples, mentioned in Fig. 4b. The figure reveals that there was a marked increase in both COF and wear rate when number of passes is raised from $i = 1$ to $i = 3$ indicating a deterioration in wear resistance. Further augmentation in number of passes to $i = 4$ produced a positive effect by reducing both studied properties while attaining five number of passes ($i = 5$) induced an augmentation in COF but a regression in wear loss. Although the surface microhardness of the burnished surface with $i = 3$ is greater compared to the

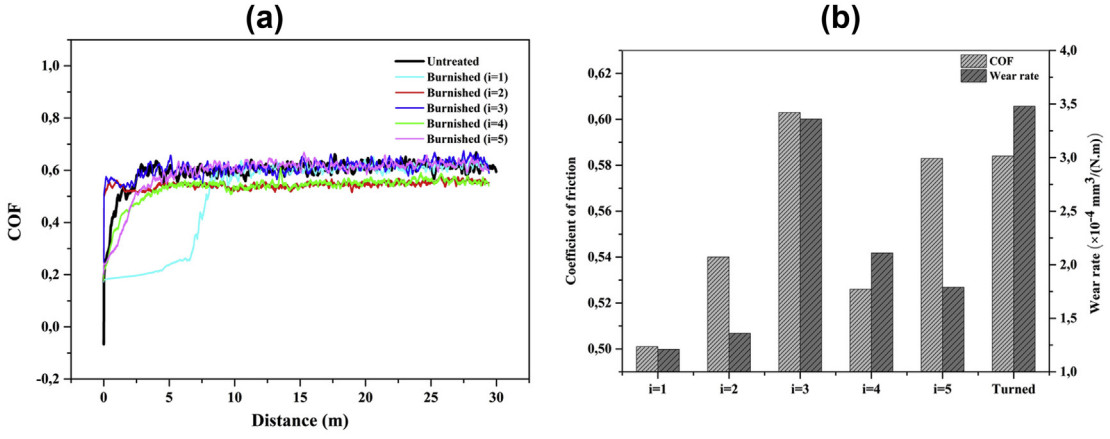



**Fig. 4 – Wear tests results for all samples: (a) COF versus sliding distance; (b) Average COF and wear rate of various samples.**

ones burnished with $i = 1$ and $i = 2$, its wear performance was lower, which can be attributed to the wear of the treated layer. Indeed, because the burnished layer was affected and totally worn out during the test of wear, the tribological behavior of the burnished surface became almost the same as the one unburnished. It can be hence proposed that the burnished layers of samples treated with $i = 4$ and $i = 5$ were partially worn out offering to them a higher wear resistance as compared to the sample burnished with $i = 3$. In order to confirm these statements, cross sectional areas of wear of all the surfaces were picked out and represented in Fig. 5. It can be clearly seen in the figure that both wear area and maximum depth of the sample burnished with one pass ($i = 1$) are the smallest what explains its best frictional behavior. In contrast, the surface burnished with three passes ($i = 3$) marked the largest wear area and equally maximum depth. For this sample, the maximum depth attained was 17.2 μm which is higher than the depth of the treated layer (15 μm) confirming therefore our suggestion reporting that the burnished layer was totally affected. This can be interpreted by the fact that each surface had shown a different evolution of microhardness beneath the surface, In that way, at the same distance from the surface, each sample represented a different value of microhardness, which determines whether the exposed layer to friction is more or less resistant. Furthermore, the maximum depths of the samples burnished with $i = 4$ and $i = 5$ were recorded as 12.2 μm and 10.9 μm respectively, which are shorter than the thicknesses of their hardened layers. Hence, during the test of wear, the consolidated layers of these samples were not totally affected which prevented the wear from spreading out to the bulk material. It can be also concluded that the depth of hardened layer of the surface burnished five times (40 μm) had offered a lower wear rate compared to the surface treated four times ($i = 4$) although they represented similar values of microhardness.

From the results presented above, it can be affirmed that the burnishing treatment, having increased the microhardness of 316L SS, also shows an effectiveness of improving its wear resistance. Compared to the turned one, all the treated surfaces are harder and consequently more resistant to friction. This is in accordance with Archard's law which states that the higher the microhardness, the more the material is resistant to wear [45]. The burnishing action is manifested by the work hardening of the surface layer which creates residual compressive stresses raising the surface microhardness. This action prevents crack growth and accordingly wear delamination [25]. It has been reported in the literature that the increase in number of passes leads to the decrease in specific wear rate because of the raise in surface microhardness which is due to condensed grain structure [6,34,46]. The present

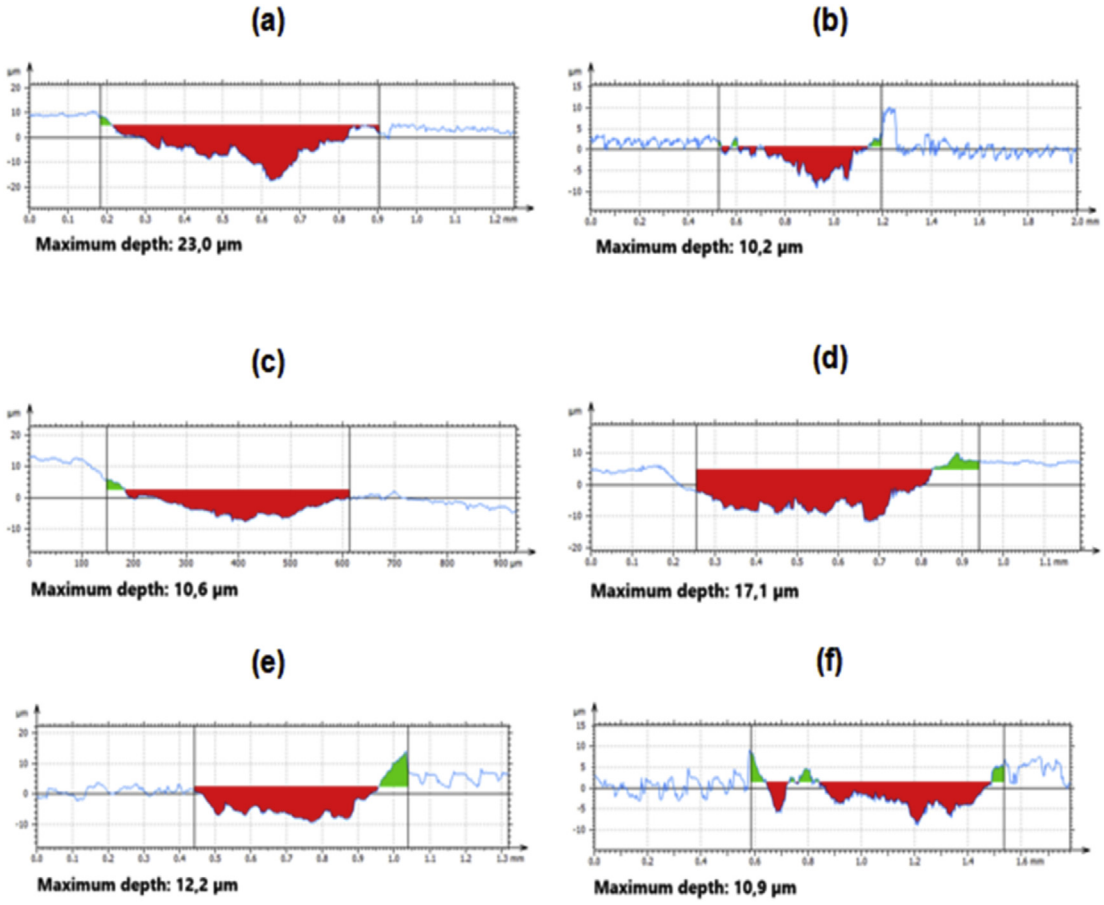



**Fig. 5 – Cross sectional areas of various worn surfaces: (a) Sample untreated; (b) burnished with $i = 1$; (c) burnished with $i = 2$; (d) burnished with $i = 3$; (e) burnished with $i = 4$; (f) burnished with $i = 5$.**

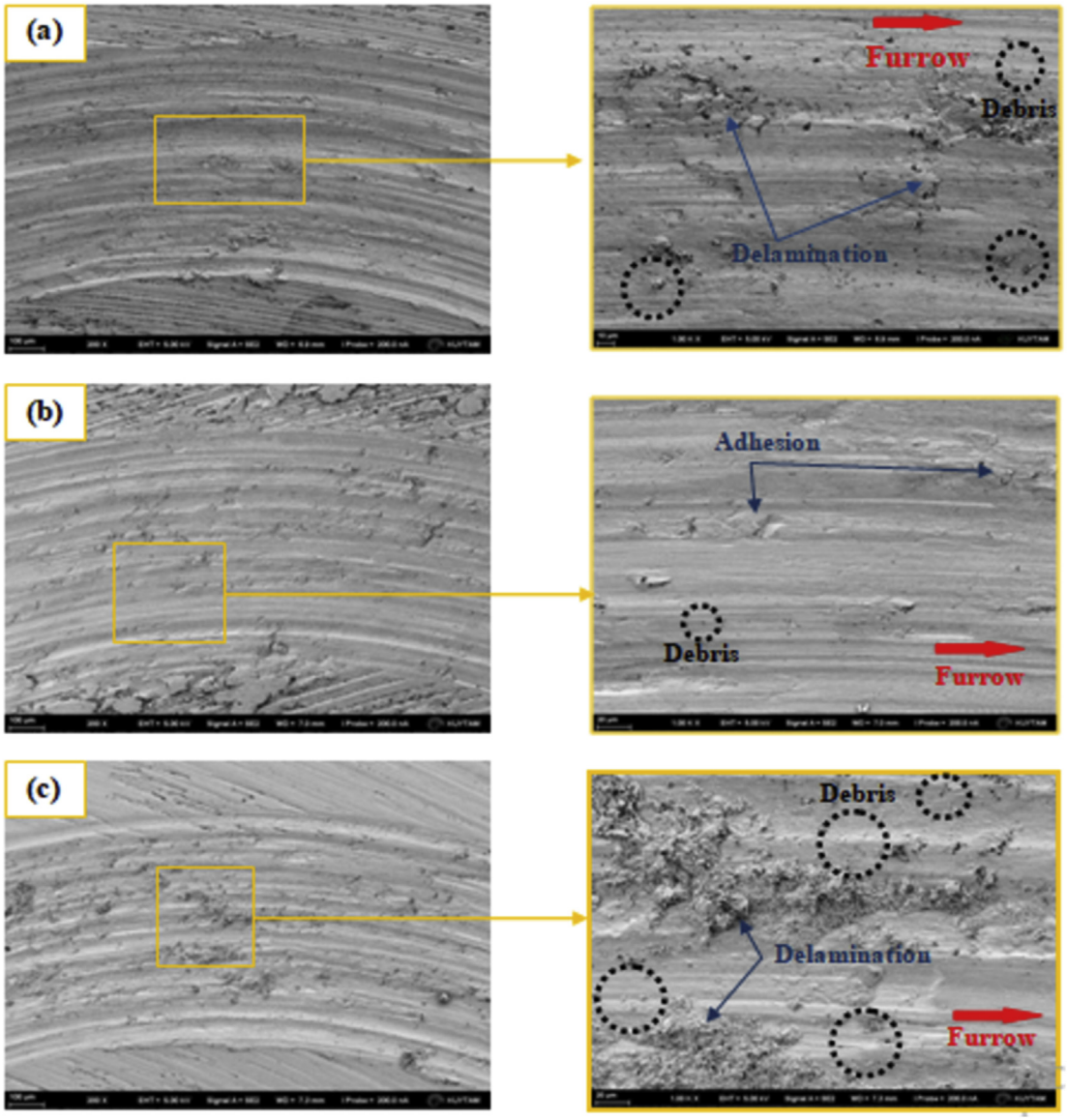



**Fig. 6 – SEM micrographs of worn surfaces: (a) Untreated; (b) burnished with $i = 1$; (c) burnished with $i = 3$.**

study shows that the impact of number of passes on frictional performance of 316L SS can be investigated through the augmentation of burnished layer depth. The repetitive passage of the ball over the surface of the 316L SS during burnishing makes it possible to deform a larger surface at a higher depth. Consequently, the distribution of microhardness across the surface will act strongly on the tribological behavior of the stainless steel.

To illustrate the wear mechanism of worn surfaces, SEM observations were performed to analyze the wear tracks of three selected samples after the wear test. Fig. 6 shows the micrographs revealed corresponding to surfaces burnished with one pass ($i = 1$) and three passes ($i = 3$) compared to the untreated one. It can be noticed from Fig. 6a that the worn surface of turned sample exhibited a severe signs of delaminations, indicating that adhesion is the dominant wear mechanism. Adhesive wear is caused by the interaction of asperities in the contact area. Under the normal load applied during wear test, the plastic deformation of the asperities occurs and creates fresh micro-junctions which will be ruptured causing the material to be transferred and eventually detached to form wear debris. After the application of ball burnishing treatment with one or three passes, adhesion still the most dominant mechanism as it is shown in Fig. 6b and c. However, there is a distinctive degree of adhesion and delamination between the three surfaces. While a regime of severe adhesive wear was predominant in the turned sample and also in the burnished one with $i = 3$, the burnished ample with ($i = 1$) exhibited a very slight adhesive wear, consistently to the views of Qin et al. [43]. The size and number of delaminations and also wear debris were estimated very high in the worn track of the surface burnished with three passes ($i = 3$) in comparison to the other surfaces. Wear debris were also detected in this surface with a high quantity as shown in

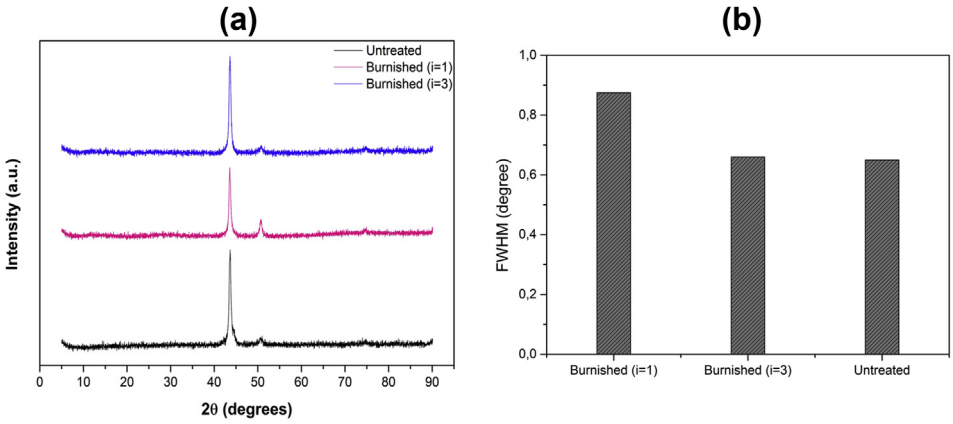



**Fig. 7 – XRD results: (a) XRD patterns of three samples; (b) FWHM values of selected samples.**

Fig. 6c. These observations explain why this sample has shown the worst frictional behavior in terms of COF and wear loss. In the wear trace of the surface burnished with one pass, only few signs of delamination with a very low size were observed, indicating that this surface has resisted strongly to the plastic deformation during wear test. This excellent wear resistance is also confirmed by the reduction of wear particles which were almost disappeared on this surface. As a result of plastic deformation, all the worn surfaces were plowed and consequently furrows and ridges were produced. The turned and also the burnished sample with $i = 3$ showed a deep furrows because of the severe wear while the sample burnished with $i = 1$ exhibited only some furrows which are very shallow. Also, it is noticed on the worn surface of burnished sample with three passes that a considerable part of material was detached during sliding and then re-deposited due to adhesion, indicating the high damage engendered on this surface as it was remarked by Dzierwa et al. [5].

Based on the above results, it can be announced that burnishing of 316L SS with fixing the optimum regime of microhardness, can significantly increase the wear performance of this material. This treatment offers to the surface an excellent resistance to plastic deformation which is provoked by contact movement during dry sliding. Definitely, burnishing makes the deformed layers very resistant to elastic and plastic deformation in contact loading, which suppresses the processes of adhesive bonding under different frictional loading [47,48].

### 3.3.4. *Phase composition analysis*

Fig. 7 shows the X-ray patterns of unburnished sample and two burnished samples: the sample burnished with one pass, and the sample burnished with three passes. These two cases were selected as they represent the highest and the lowest wear resistance respectively. It can be seen that all the patterns have two clear peaks at 43.5° and 50.7° and a very small one at 74.6° which are associated with the face cubic centered crystalline structure (γ phase), indicating that BB had not provoked any change in phase composition of 316L SS. However, the diffraction peak intensities were weakened and broadened for the sample burnished with one pass while they remain almost unchanged for the sample burnished with three passes in comparison to the untreated sample. XRD analysis was also used to evaluate any change in grain size because of BB process. Fig. 7b represents the values of the full width at half maximum (FWHM) measured from the primary peaks. This parameter permit to analyze the surface state of the material as it is related to grain distortion, density of dislocations and residual stresses [49]. Compared to the untreated sample, the FWHM of burnished samples was increased indicating that BB treatment had provoked a decrease in the grain size [49]. The FWMH of the burnished sample with $i = 1$ was notably raised whereas the one of the burnished sample with $i = 3$ was very slightly increased indicating a better grain refinement in the first case. The effect of ball burnishing on the grain size is in fact reasonable since this process lead to the acceleration of the motion of dislocations [49]. It has been outlined by Lang et al. [39] that surface nanocrystallization of 316L SS produced the grains refinement, by which the microhardness was enhanced according to Hall–Petch theory, which suggests a strengthened relationship between hardness and grain size. Wang et al. [40] have also ascribed the increment in hardness of Ti–6Al–4V titanium alloy by the grain refinement produced by ultrasonic surface rolling. Therefore, it can be confirmed that the decrement in grain size obtained after ball burnishing of 316L SS could raise the microhardness of the material, which influenced very positively on its frictional behavior.

## 4. Conclusions

Based on the experimental results, valuable information about the influence of ball burnishing process on 316L SS have been delivered. The major conclusions are outlined as:

1 A successful increment of microhardness has been obtained after BB treatment. The optimum parameters set as $P_x = 87$ N, $f = 0.18$ mm/rev, $D = 13$ mm, and $i = 1$ has proved an important increase in the microhardness by more than 100 Hv. Nevertheless, the strain hardening induced by BB was limited to only 15 μm beneath the surface which is due to high feed rate and low load applied.

2 The number of passes have shown an advantageous impact on the microhardness which microhardness was increased from 447.3 Hv for one pass to 593.0 Hv for five passes. Even so, the depth of burnished layer was restricted to only 40 μm. It is worth noting that no saturation effect was observed due to the application of appropriate parameters (*Px* and *f*) during the process.
3 The mechanical properties of the surface and the sub-surface of 316L SS were highly influenced by the number of passes. When the latter are increased, both the nano-hardness and the elastic modulus have been increased from 4.42 to 5.91 GPa and from 189.5 to 219.9 GPa, respectively. This effect was favored by the cold work induced on the sample during the BB treatment.
4 Ball burnishing must be recommended to strengthen the frictional performance of 316L SS as it has reduced its coefficient of friction with 8.57% and its wear loss by up to 65.2%.
5 The number of passes is not influential in terms of tribological behavior improvement as the results have indicated that one pass is the most effective for reducing the COF and the wear loss. Nevertheless, as the depth of the burnished layer increases, the sub-surface layers could be protected from wearing-out.
6 The phases composition of 316L SS was not affected by BB but a grain refinement was produced indicating that condensed structure and residual stresses were induced.
7. In perspective study, other functional properties of 316L, such as its fatigue endurance and corrosion resistance, after the selected regime of BB should be investigated.

## Declaration of Competing Interest

The authors declare that they have no conflicts of interest.

## Abbreviations

| | |
|---|---|
| BB | Ball Burnishing |
| RSM | Response Surface Method |
| SS | Stainless Steel |
| $f_t$ | Turning Feed Rate [mm/rev] |
| $p$ | Depth of Pass [mm] |
| $N$ | Rotational Frequency [rev/min] |
| $P_x$ | Burnishing Force [N] |
| $f$ | Burnishing Feed Rate[mm/rev] |
| $D$ | Ball Diameter [mm] |
| i | Number of Burnishing Passes |
| COF | Coefficient of Friction |

## REFERENCES


[1] Hwang JS, Mehta AD, Yoon RS, Beebe KS. From amputation to limb salvage reconstruction: evolution and role of the endoprosthesis in musculoskeletal oncology. J Orthop Traumatol 2014;15:81–6.
[2] Attabi S, Himour A, Laouar L, Motallebzadeh A. Effect of ball burnishing on surface roughness and wear of AISI 316L SS. J Bio- Tribo-Corros 2021;7(7).
[3] Kurgan N, Varol R. Mechanical properties of P/M 316L stainless steel materials. Powder Technol 2010;201:242–7.
[4] Wilches LV, Uribe JA, Toro A. Wear of materials used for artificial joints in total hip replacements. Wear 2008;265:143–9.
[5] Dzierwa A, Gałda L, Tupaj M, Dudek K. Investigation of wear resistance of selected materials after slide burnishing process. Eksploat Niezawodn 2020;22(3):432–9.
[6] Revankar GD, Shetty R, Rao SS, Gaitonde VN. Wear resistance enhancement of titanium alloy (Ti–6Al–4V) by ball burnishing process. J Mater Res Technol 2016;6(1):13–32.
[7] Avilés R, Albizuri J, Rodríguez A, De Lacalle LL. Influence of low-plasticity ball burnishing on the high-cycle fatigue strength of medium carbon AISI 1045 steel. Int J Fatigue 2013;55:230–44.
[8] Sadeler R, Corak S, Atasoy S, Bulbul F. Evaluation of an electroless nickel-boron (Ni-B) coating on corrosion fatigue performance of ball burnished AISI 1045 steel. Kovove Mater 2013;51(6):351–6.
[9] Patel PN, Patel NB, Patel TM. Parametric optimization of ball burnishing process parameter for hardness of aluminium alloy 6061. IOSR J Eng 2014;4:21–6.
[10] Revankar GD, Shetty R, Rao SS, Gaitonde VN. Analysis of surface roughness and hardness in ball burnishing of titanium alloy. Measurement 2014;58:256–68.
[11] Dimitrov DM, Slavov SD, Dimitrov Z. Experimental research on the effect of the ball burnishing process, using new kinematical scheme on hardness and phase composition of surface layer of AISI 304L stainless steel. MATEC Web of Conferences 2017;112:02001.
[12] Teimouri R, Amini S, Bami AB. Evaluation of optimized surface properties and residual stress in ultrasonic assisted ball burnishing of AA6061-T6. Measurement 2018;116:129–39. https://doi.org/10.1016/j.measurement.2017.11.001.
[13] Jerez-Mesa R, Travieso-Rodríguez JA, Landon Y, Dessein G, Lluma-Fuentes J, Wagner V. Comprehensive analysis of surface integrity modification of ball-end milled Ti-6Al-4V surfaces through vibration-assisted ball burnishing. J Mater Process Technol 2019;267:230–40.
[14] Świrad S, Wydrzynski D, Nieslony P, Krolczyk GM. Influence of hydrostatic burnishing strategy on the surface topography of martensitic steel. Measurement 2019;138:590–601.
[15] Silva-Álvarez DF, Márquez-Herrera A, Saldana-Robles A, Zapata-Torres M, Mis-Fernández R, Pena-Chapa JL, et al. Improving the surface integrity of the CoCrMo alloy by the ball burnishing technique. J Mater Res Technol 2020;9(4):7592–601.
[16] Nguyen TT, Cao LH, Nguyen TA, Dang XP. Multi-response optimization of the roller burnishing process in terms of energy consumption and product quality. J Clean Prod 2019;245:119328.
[17] Basak HM, Ozkan T, Toktaset I. Experimental research and ANN Modeling on the impact of the ball burnishing process on the mechanical properties of 5083 Al-Mg material sheets through vibration-assisted ball burnishing. Kovove Mater 2019;57(1):61–74.
[18] Kalisz J, Zak K, ˙Wojciechowski S, Gupta MK, Krolczyk GM. Technological and tribological aspects of milling-burnishing process of complex surfaces. Tribol Int 2020;155:106770.
[19] Cagan SC, Pruncu CI, Buldum BB. An investigation into ball burnishing process of magnesium alloy on CNC lathe using different environments. J Magnes Alloys 2020;8(4):1061–70.
[20] Charfeddine Y, Youssef S, Sghaier S, Sghaier J, Hamdi H. Study of the simultaneous Grinding/Ball-burnishing of AISI

4140 based on finite element simulations and experiments. Int J Mech Sci 2020;192:106097.
[21] Jerez-Mesa R, Fargas G, Josep Roa J, Llumà J, Travieso-Rodriguez JA. Superficial effects of ball burnishing on TRIP steel AISI 301LN sheets. Metals 2021;11:82.
[22] Lee SSG, Tam SC, Loh NH. Ball burnishing of 316L stainless steel. J Mater Process Technol 1993;37:241–51.
[23] Yilmaz H, Sadeler R. Effect of ball burnishing treatment on the fatigue behavior of 316L stainless steel operating under anodic and cathodic polarization potentials. Metall Mater Trans A 2018;49:5393–401.
[24] Gulhane UD, Mishra SB, Mishz PK. Enhancement of surface roughness of 316L stainless steel and Ti-6Al-4V using low plasticity burnishing: DOE approach. Int J Mech Eng Technol 2012;3:150–60.
[25] Tanaka H, Ishii W, Yanagi K. Optimal burnishing conditions and mechanical properties of surface layer by surface modification effect induced of applying burnishing process to stainless steel and aluminum alloy. J Jpn Soc Technol Plast 2011;52:726–30.
[26] Salmi M, Huuki J, Ituarte IF. The ultrasonic burnishing of cobalt-chrome and stainless steel surface made by additive manufacturing. Prog Addit Manuf 2017;2:31–41.
[27] Goupy J. Plans d'expériences pour surfaces de réponse. Paris: Dunod; 1999.
[28] Bourebia M, Laouar L, Hamadache H, Dominiak S. Improvement of surface finish by ball burnishing: approach by fractal dimension. Surf Eng 2017;33:255–62.
[29] Yuan XL, Sun YW, Gao LS, Jiang SL. Effect of roller burnishing process parameters on the surface roughness and microhardness for TA2 alloy. Int J Adv Manuf Technol 2015:1–11.
[30] Laouar L, Hamadache H, Saad S, Bouchelaghem A, Mekhilef S. Mechanical surface treatment of steel-Optimization parameters of regime. Phys Procedia 2009;2:1213–21.
[31] Spiegel MR. Probabilité et statistique. Paris: Series Schaum; 1983.
[32] Nguyen TT, Le XB. Optimization of interior roller burnishing process for improving surface quality. Mater Manuf Process 2018;33(11).
[33] Hassan AM. The effects of ball- and roller-burnishing on the surface roughness and hardness of some non-ferrous metals. J Mater Process Technol 1997;72:385–91.
[34] El-Taweel TA, El-Axir MH. Analysis and optimization of the ball burnishing process through the Taguchi technique. Int J Adv Manuf Technol 2009;41:301–10.
[35] Hassan AM, Al-Jalil HF, Ebied AA. Burnishing force and number of tool passes for the optimum surface finish of brass components. J Mater Process Technol 1998;83:176–9.
[36] Nemat M, Lyons AC. An investigation of the surface topography of ball burnished mild steel and aluminium. Int J Adv Manuf Technol 2000;16:469–73.
[37] Klocke F, Backer V, Wegner H, Feldhaus B, Baron H, Hessert R. Influence of process and geometry parameters on the surface layer state after roller burnishing of IN718. Prod Eng Res Dev 2009;3:391–9.
[38] Warren AW, Guo YB, Weaver ML. The influence of machining induced residual stress and phase transformation on the measurement of subsurface mechanical behavior using nanoindentation. Surf Coat Technol 2006;200:3459–67.
[39] Lang FC, Xing YM, Zhu J, Zhao YR. Study of the mechanical properties of a nanostructured surface layer on 316L stainless steel. Adv Mater Sci Eng 2016:7517616.
[40] Wang Z, Xiao Z, Huang C, Wen L, Zhang W. Influence of ultrasonic surface rolling on microstructure and wear behavior of selective laser melted Ti-6Al-4V alloy. Materials 2017;10:1203.
[41] Fellah M, Labaïz M, Assala O, Iost A, Dekhil L. Tribological behaviour of AISI 316L stainless steel for biomedical applications. Tribol Mater Surf Interfaces 2016;7:135–49.
[42] Yasuhiro M, Kei D. Surface age hardening and wear properties of beta-type titanium alloy by laser surface solution treatment. Mater Trans 2011;52(4):714–8.
[43] Qin W, Kang J, Li J, Yue W, Liu Y, She D, et al. Tribological behavior of the 316L stainless steel with heterogeneous lamella structure. Materials 2018;11:1839.
[44] El-Tayeb NSM, Low KO, Brevern PV. Enhancement of surface quality and tribological properties using ball burnishing process. Mach Sci Technol 2008;12:234–48.
[45] Archard JF. Contact and rubbing of flat surfaces. J Appl Phys 1953;24:981–8.
[46] Bressan JD, Hesse R. Construction and validation tests of pin-on-disc equipment. In: XVI Congresso Brasileiro de Engenharia Mecânica, COBEM 2001; 2001.
[47] Kuznetsov VP, Makarov AV, Psakhie SG, Savrai RA, Malygina IYu, Davydova NA. Tribological aspects in nanostructuring burnishing of structural steels. Phys Mesomech 2014;17:250–64.
[48] Xu X, Liu D, Zhang X, Liu C, Liu D. Mechanical and corrosion fatigue behaviors of gradient structured 7B50-T7751 aluminum alloy processed via ultrasonic surface rolling. J Mater Sci Technol 2019;40(1):88–98.
[49] Sua H, Shena X, Xua CH, He J, Wang B, Sua G. Surface characteristics and corrosion behavior of TC11 titanium alloy strengthened by ultrasonic roller burnishing at room and medium temperature. J Mater Res Technol 2020;9(4):8172–85.